Propagation of Hydrodynamic Interactions in Colloidal Suspensions

Stuart Henderson, Steven Mitchell, and Paul Bartlett*

School of Chemistry, University of Bristol, Bristol BS8 1TS, United Kingdom
(Received 14 September 2001; published 8 February 2002)

We describe direct measurements of the dynamics of two colloidal spheres before hydrodynamic interactions have had time to fully develop. We find that the dynamics of the two spheres are coupled at times significantly shorter than τ_ν, the time required for vorticity to diffuse between the two spheres. From the distance dependence of the measured coupling, we infer that hydrodynamic interactions develop in a sonic time scale.

Hydrodynamic forces are of central importance in many areas of chemical physics, material science, and engineering. Yet despite their scientific significance and technological relevance, our understanding of hydrodynamic interactions is still far from complete and is capable of surprises [1]. In recent years several apparently conflicting theories and experiments have been reported [2–8] describing the mechanism by which such forces are transmitted between different particles. In this Letter we describe measurements of the short-time dynamics of two colloidal spheres which probe directly the temporal development of hydrodynamic interactions. We show that sound plays a crucial role in their development.

A particle set into motion by a random thermal fluctuation or an external force transfers momentum to a neighboring particle via two mechanisms which generally operate on very different time scales. For a neutrally buoyant particle $1/3$ of the initial momentum is carried off rapidly by a spherical sound wave whose front arrives at a neighboring particle, a distance r away, after a time $\tau_s = r/c$, where c is the speed of sound in the fluid. After the sound wave has separated a vortex ring develops around the particle. The region of vorticity grows diffusively, as the remaining momentum is distributed over larger and larger volumes, with the disturbance taking a time of order $\tau_\nu = r^2/\nu$ to reach a neighboring particle, where ν is the kinematic viscosity of the fluid. The relative importance of the two mechanisms varies with the length scale r. For an *isolated* colloidal sphere of radius $a \simeq 0.5$ μm the sonic time τ_s (with $r = a$) is of order 0.1 ns so that on experimental time scales the sound mode is largely irrelevant. Because of this the tacit assumption has been, until recently, that hydrodynamic interactions between *different* particles are also largely unaffected by sound effects and so develop on the time scale τ_ν of vorticity diffusion. Hence, it came as a great surprise when diffusing wave spectroscopy (DWS) experiments [2] observed an apparent scaling behavior for the time-dependent self-diffusion constant $D(t)$ which suggested that even for $t < \tau_\nu$ a suspension behaved as an "effective" medium with a viscosity equal to the suspension viscosity. This scaling is puzzling since, if hydrodynamics

propagate by vorticity diffusion, for $t < \tau_\nu$ there is not enough time for vorticity to travel the typical distance between particles. Particles should therefore move independently of each other and the relevant viscosity would be expected to be that of the suspending solvent and not the suspension. These conjectures led Espanol and co-workers [5,6] to suggest that hydrodynamic interactions might develop on a sonic rather than a vorticity time scale and so effective fluid behavior could be seen for $t < \tau_\nu$. However, careful numerical simulations [7] and theoretical work [8] have shown that the apparent scaling of $D(t)$ observed in the experiments actually occurs only on a longer time scale, $t \gtrsim 4\tau_\nu$, and hence there is no need to introduce a sonic mechanism. While sound has also been invoked to explain discrepancies seen between DWS measurements of collective diffusion and simulations [9], there is currently no clear experimental evidence of the role that sound plays, if any, in establishing hydrodynamic interactions.

In this Letter, we describe experimental measurements of the time-dependent hydrodynamic forces in the simplest coupled Brownian system, two spheres of radius a separated by a distance $\rho = r/a$ and suspended in a solvent of kinematic viscosity ν. We use a pair of optical tweezers to position the two spheres within the sample volume and a laser deflection technique to track the in-plane motion of both spheres with a time resolution of 50 μsec and a precision approaching 1 nm. By positioning the two spheres well apart the characteristic time, $\tau_\nu = r^2/\nu$, for vorticity to diffuse between the two spheres is sufficiently lengthened that our measurements probe hydrodynamic interactions at times substantially shorter than τ_ν. We find that the trajectories of the two spheres are still correlated at $t < \tau_\nu$. By varying the separation between the two particles, we confirm that this short-time correlation arises from sound propagation.

The measurements were performed on single poly(methyl methacrylate) spheres selected from a suspension of radius $a = 0.652 \pm 0.039$ μm. The spheres were coated with a ~10 nm thick layer of the copolymer poly(methyl methacrylate)-poly(12-hydroxy stearic acid) and suspended in a mixture of cyclohexane and

cis-decalin of viscosity $\eta = 1.217$ mPas and density $d = 0.808$ gm cm^{-3}. Previous experiments have shown that, under these conditions, the interparticle potential is close to hard sphere. A dilute suspension of spheres was loaded into the interior of a rectangular glass capillary of area 5×0.3 cm and thickness 170 μm which was hermetically sealed with a rapid setting adhesive. The Brownian dynamics of the two spheres were studied using a dual-beam optical tweezer setup, similar to that described by Meiners and Quake [10]. Two optical traps were created by directing collimated orthogonal-polarized beams from a Nd-YAG laser, producing $\sim$100 mW of 1064 nm radiation, into the back focal plane of a 100×1.3 NA oil-immersion objective lens. The resulting optical gradient forces are strong enough to localize a sphere near each beam focus. For small excursions of the sphere from the trap center, the restoring force was found to be linear in displacement, with a force constant k which varied linearly with the laser power. The intensity of each beam was carefully adjusted to ensure that the strength of the two optical traps differed by less than 5%. Although the laser beam fixed the average position of each sphere, random Brownian forces caused small but measurable fluctuations in the instantaneous location of each sphere. These position fluctuations were measured by recording the interference between the forward scattered light and the transmitted laser beam in the back focal plane of the microscope objective with a pair of quadrant photodetectors. Custom-built current-to-voltage converters enabled the in-plane positions of both spheres to be recorded with a 1 nm spatial resolution at 50 μsec intervals. The stiffness k of each trap was found by fitting the mean-squared displacement $\langle \Delta x^2(t) \rangle$ of an isolated single sphere to $\langle \Delta x^2(t) \rangle = \langle \Delta x^2 \rangle_\infty [1 - \exp(-t/\tau)]$ where the harmonic time, $\tau = \xi_0/k$, is the ratio of the single particle friction coefficient ($\xi_0 = 6\pi\eta a$) to the trap stiffness and $\langle \Delta x^2 \rangle_\infty = 2k_B T/k$; here the brackets indicate ensemble averages. Typical values for k were of the order of 5.1×10^{-6} N m^{-1}, which equates to a root-mean-square fluctuation in position of ca. 40 nm. This is sufficiently small in comparison with typical sphere spacings ($r > 2.5$ μm) that the spheres dynamics are recorded essentially at a constant pair separation. The mean spacing r between the two spheres was adjusted from between 2.5 and 20 μm in roughly 2.5 μm increments, taking care to ensure that at each separation both spheres were at least 40 μm away from any wall, to reduce boundary effects. At each pair separation data were collected for about 500 s to yield in excess of 8×10^6 coordinate pairs.

To characterize how the trajectory of one particle is affected by the motion of its neighbor we calculated a dimensionless collective diffusion constant, $D_c(\rho, t) = \langle \Delta x_1(t) \Delta x_2(t) \rangle / 2D_0 t$, where $\Delta x_1(t) = x_1(t) - x_1(0)$ is the displacement of particle 1 parallel to the pair separation vector $\mathbf{r} = \mathbf{r}_2 - \mathbf{r}_1$, and $D_0 = k_B T/\xi_0$ is the diffusion constant of an isolated sphere. For long times, $t \gg \tau_\nu$, when hydrodynamic interactions between the two spheres are fully developed, the strength of the mutual coupling, measured by D_c, will vary inversely with the pair separation. Consequently, the scaled diffusion constant $\rho D_c(\rho, t)$ should fall on a single master curve when plotted against t/τ. Deviations from scaling reveal the presence of time-dependent hydrodynamic forces. Figure 1 shows typical data for four different separations which reveal significant differences. In particular, the values of ρD_c measured at short times are seen as larger for the closest pair (a) than for the well separated particle pair (d). These quantitative differences indicate that, at short times, hydrodynamic interactions are *screened,* in the sense that they decay more rapidly than the usual $1/\rho$ dependence expected.

To understand the origin of time-dependent screening, we analyzed our data to yield the two-particle friction coefficients. The stochastic motion of two small neutrally buoyant particles in a fluid may be described by means of a generalized Langevin equation, which in the complex frequency plane reads

$$i\omega m U_m(\omega) = -\sum_{n=1}^{2} \xi_{mn}(\omega) U_n(\omega)$$
$$- \frac{k}{i\omega} U_m(\omega) + f_m(\omega), \qquad (1)$$

where m is the particle mass and $U_m(\omega)$ is the Fourier-Laplace transform of the particle velocity, $\int_0^\infty dt \exp(-i\omega t) U_m(t)$. The fluctuating particle velocities are driven by frequency-dependent random
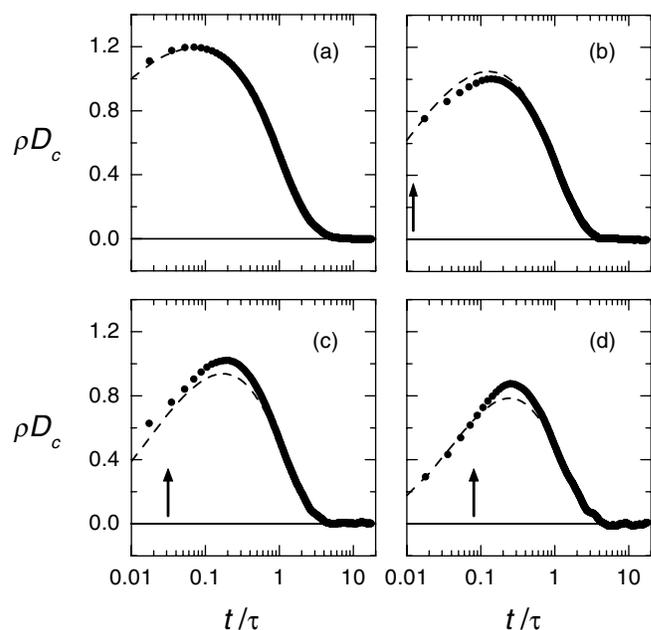

FIG. 1. The time evolution of the scaled diffusion constant $\rho D_c(\rho, t)$ measured at pair separations ρ of (a) 4.72, (b) 11.41, (c) 17.59, and (d) 28.94. The time is scaled by the optical-trap time constant τ. The arrows label the time τ_ν for vorticity to diffuse between the two spheres. The dashed curve through the data is the prediction of the theory described here, Eqs. (2) and (5).

forces $f_m(\omega)$, the spectral density of which is, from the fluctuation-dissipation theorem, related to the frequency-dependent friction coefficient $\xi_{mn}(\omega)$ between particles m and n by the expression $\langle f_m(\omega)f_n(\omega')^*\rangle = 4\pi k_B T \, \mathrm{Re}[\xi_{mn}(\omega)]\delta(\omega - \omega')$ [11]. The coupled Langevin equation (1) is solved by introducing independent collective and relative modes of motion and using standard techniques [11] to evaluate the velocity correlation functions and hence the joint mean square displacement $\langle \Delta x_1(t)\Delta x_2(t)\rangle$. If inertial terms are ignored, which is valid at all but the highest frequencies, the solution is

$$\langle \Delta x_1(\omega)\Delta x_2(\omega)\rangle$$
$$= \frac{-2k_B T\xi_{12}(\omega)}{k^2 + 2i\omega k\xi_{11}(\omega) - \omega^2[\xi_{11}^2(\omega) - \xi_{12}^2(\omega)]}.$$
(2)

At large pair separations this solution may be further simplified since the self-friction $\xi_{11}(\omega)$ will not vary significantly with the pair separation and so may be approximated, with negligible error, by the single particle result [12], $\xi_{11}(\omega) = \xi_0(1 + \alpha a)$, where $\alpha = \sqrt{i\omega/\nu}$ and $\mathrm{Re}\,\alpha > 0$. If we further assume that the joint friction $|\xi_{12}(\omega)|$ is small in comparison with $|\xi_{11}(\omega)|$ (a result which is justified since the ratio of the two friction coefficients is of order $1/\rho$ or less) Eq. (2) reduces to an expression for $\xi_{12}(\omega)$ in terms of the Fourier-Laplace transform of the joint displacement,

$$\frac{\xi_{12}(\omega)}{\xi_0} = -\frac{[1 + i\omega\tau(1 + \alpha a)]^2}{2D_0\tau^2}\langle \Delta x_1(\omega)\Delta x_2(\omega)\rangle.$$
(3)

The transform was calculated numerically in two stages. First, a series of smoothed cubic polynomial splines was fitted to the data. Then the contribution to the transform from each time interval was formally written in terms of incomplete gamma functions which were evaluated numerically and summed. Tests showed that errors in the transform were of the order of 5%, except near the frequency extremes where truncation errors became more significant.

Figure 2 shows a selection of the experimental two-particle friction coefficients measured at three different pair separations and plotted as a function of the scaled frequency $\omega\tau_\nu$. The friction coefficients are clearly frequency dependent, reflecting the temporal development of the hydrodynamic interaction forces. A close examination reveals that the sensitivity of $\xi_{12}(\omega)$ to increasing frequency varies markedly with the sphere separation, with the more widely separated particle pairs showing a proportionately greater decrease with increasing frequency. To explore the nature of this dependence in greater detail, we plot in Fig. 3 the variation with separation of the friction coefficient $\xi_{12}(\omega)$, at a *constant* frequency ω. At a low frequency, $\omega = 350 \text{ rad s}^{-1}$, where the friction coefficient does not change markedly with frequency, Fig. 3 reveals

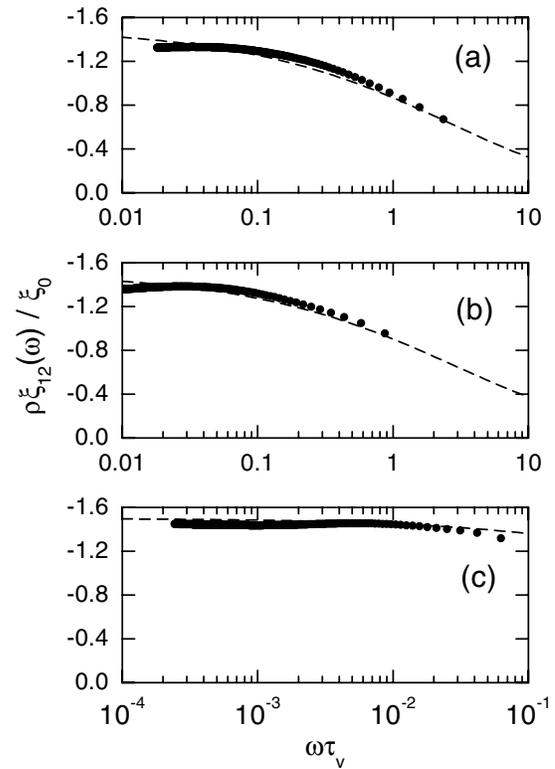FIG. 2. The frequency-dependent two-particle friction coefficients (circles) measured at separations ρ of (a) 28.94, (b) 17.59, and (c) 4.72. The frequencies are scaled by the vorticity diffusion time τ_ν. The dashed lines are the predictions of Eq. (5), with no adjustable parameters. Note the close agreement.

that ξ_{12} shows the usual $1/\rho$ dependence on pair separation. By contrast at a higher frequency, $\omega = 10^5 \text{ rad s}^{-1}$, the decay is seen to be significantly faster than $1/\rho$ with the data approaching asymptotically a limiting $1/\rho^3$ variation. This striking *qualitative* difference between the low and the high frequency behavior highlights a change in the mechanism of hydrodynamic coupling with time.

To interpret these observations we approximate the velocity field around a given sphere by the flow induced by a pointlike force at the particle center. The time-dependent Green's function for the velocity field at **r** following a sudden unit impulse applied at the origin was first calculated by Oseen in 1927 [12] as

$$\mathbf{G}(\mathbf{r}, t) = \frac{e^{-r^2/4\nu t}}{d(4\pi\nu t)^{3/2}}\left[\left(1 + 2\frac{\nu t}{r^2}\right)\mathbf{I} - \left(1 + 6\frac{\nu t}{r^2}\right)\hat{r}\hat{r}\right]$$
$$+ \frac{\Phi(r/\sqrt{4\nu t})}{4\pi dr^3}[3\hat{r}\hat{r} - \mathbf{I}],$$
(4)

where $\Phi(x)$ is the error function. The first term in this equation details the time-dependent flows generated as vorticity diffuses radially out from the origin while the second dipolar term is due to the spherical sound wave which, since the fluid is assumed incompressible, propagates instantaneously. In the limit $t \to 0$ of Eq. (4) only the last term, the sound mode, survives so that the flow field is instantaneously long ranged [12], decaying as $\sim 1/r^3$. A neighboring sphere tracks the temporal development of
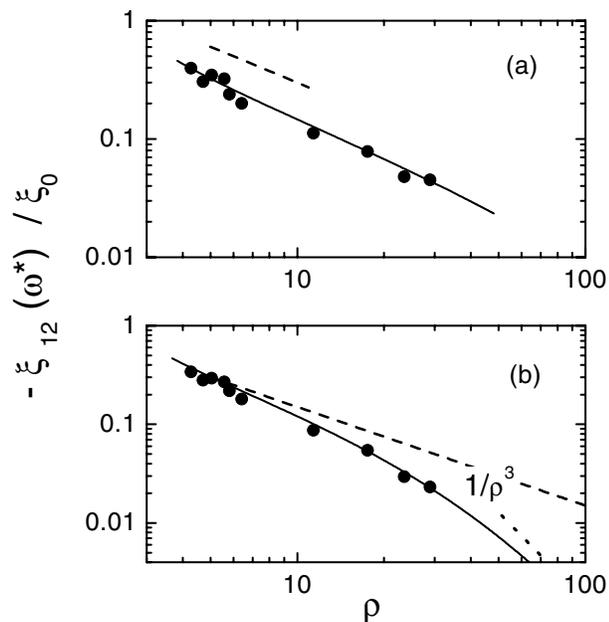
FIG. 3. The dependence on the pair separation ρ of the two-particle friction coefficients (circles) measured at a fixed frequency $\omega*$ of (a) 350 rad s^{-1}, and (b) 10^5 rad s^{-1}. The dashed and dotted lines correspond to limiting $1/\rho$ and $1/\rho^3$ decays, respectively. The solid line is the theoretical prediction of Eq. (5).

the fluid velocity. At large separations, where the spheres are well approximated by points, the two-particle mobility tensor $\boldsymbol{\mu}(\boldsymbol{r}, t)$ is equal to the Green's function $\boldsymbol{G}(\boldsymbol{r}, t)$. Taking the Fourier-Laplace transform of $\boldsymbol{G}(\boldsymbol{r}, t)$ yields the frequency spectrum of the two-particle mobility. Inverting this tensor gives the following simple expression for the frequency-dependent joint friction coefficient, parallel to $\boldsymbol{r}$,

$$\frac{\xi_{12}(\omega)}{\xi_0} = -\frac{3a}{\alpha^2 r^3}\left[1 - (\alpha r + 1)e^{-\alpha r}\right] + \mathcal{O}(\alpha^2 a^2).$$

(5)

The self-friction coefficient, in the same limit, is the isolated single particle result, $\xi_{11}(\omega) = \xi_0(1 + \alpha a)$. Taking the limit $\omega \to 0$ in Eq. (5) we recover the usual Oseen approximation to the longitudinal friction coefficient, $\lim_{\omega \to 0}\xi_{12}(\omega)/\xi_0 = -(3/2)\rho^{-1}$, with the coefficient decaying inversely with pair separation. At short times, as we have seen, the velocity field is dominated by the sound mode. The Green's function parallel to $\boldsymbol{r}$ is then asymptotically $\sim \Phi(r/\sqrt{4\nu t})/(2\pi d r^3)$ so that the high-frequency limit of the friction coefficient is expected to vary as the inverse cube of the pair separation, $\lim_{\omega \to \infty}\xi_{12}(\omega)/\xi_0 = -(3/\alpha^2 a^2)\rho^{-3}$. The $1/\rho^3$ decay observed in Fig. 3 can therefore be ascribed to hydrodynamic coupling caused by sound propagation. The full expression for $\xi_{12}(\omega)$ is plotted as the solid curves in Figs. 2 and 3 and is seen to fit the data rather well confirming the accuracy of this picture.

Our results confirm the suggestion of Espanol and co-workers [5,6] that hydrodynamic interactions are established on the speed of sound. Furthermore, we see that for times comparable with the decay of particle velocities the dominant effect on collective diffusion is the sound mode; the diffusive propagation of vorticity plays only a second role. This is in marked contrast to the situation in self-diffusion where vorticity diffusion dominates. Although this observation would seem to imply that a full compressible theory is required to provide a complete understanding of hydrodynamic interactions, comparison between our results and a simple incompressible theory indicates, at least on the time scales of our experiments, that the effects of sound propagation can be understood quite simply.

In conclusion, we have verified experimentally that colloidal particles are coupled hydrodynamically on time scales significantly shorter than τ_ν, the time taken for vorticity to diffuse between the spheres. At times $t \ll \tau_\nu$ we find that the strength of the hydrodynamics interactions between particles is screened and varies asymptotically as $1/r^3$ which suggests that the mechanism linking the velocities of neighboring particles is sound propagation. Quantitative agreement between our measurements and an incompressible theory supports this interpretation. In future work, we intend to explore the role of sound propagation in concentrated suspensions using similar single particle techniques but with an index-matched host suspension.

*Electronic address: P.Bartlett@bristol.ac.uk
[1] T. M. Squires and M. P. Brenner, Phys. Rev. Lett. **85**, 4976 (2000).
[2] J. X. Zhu, D. J. Durian, J. Muller, D. A. Weitz, and D. J. Pine, Phys. Rev. Lett. **68**, 2559 (1992).
[3] M. H. Kao, A. G. Yodh, and D. J. Pine, Phys. Rev. Lett. **70**, 242 (1993).
[4] A. J. C. Ladd, Phys. Rev. Lett. **70**, 1339 (1993); J. Fluid Mech. **271**, 311 (1994).
[5] P. Espanol, M. A. Rubio, and I. Zuniga, Phys. Rev. E **51**, 803 (1995).
[6] P. Espanol, Physica (Amsterdam) **214A**, 185 (1995).
[7] C. P. Lowe and D. Frenkel, Phys. Rev. E **54**, 2704 (1996).
[8] H. J. H. Clercx, Phys. Rev. E **56**, 2950 (1997).
[9] A. J. C. Ladd, H. Gang, J. X. Zhu, and D. A. Weitz, Phys. Rev. Lett. **74**, 318 (1995); Phys. Rev. E **52**, 6550 (1995).
[10] J.-C. Meiners and S. R. Quake, Phys. Rev. Lett. **82**, 2211 (1999).
[11] R. Kubo, M. Toda, and N. Hashitsume, *Statistical Physics II* (Springer-Verlag, Berlin, 1978).
[12] B. Cichocki and B. Felderhof, Phys. Rev. E **62**, 5383 (2000).